

## PLC-BASED MONITORING AND CONTROL OF DISTRIBUTED GENERATION AND STORAGE SYSTEMS IN LV SMART GRIDS: ARCHITECTURE, DEVICES AND CHANNEL CHARACTERIZATION TOOLS

G. Artale <sup>(1)</sup>, G. Caravello <sup>(1)</sup>, A. Cataliotti <sup>(1)</sup>, V. Cosentino <sup>(1)</sup>, D. Di Cara <sup>(2)</sup>, V. Ditta <sup>(1)</sup>,  
S. Guaiana <sup>(2)</sup>, N. Panzavecchia <sup>(2)</sup>, G. Tinè <sup>(2)</sup>

<sup>(1)</sup>Dep. of Engineering, University of Palermo, Palermo, Italy

<sup>(2)</sup>National Research Council (CNR), Institute of Marine Engineering (INM), Palermo, Italy  
mail autore di riferimento: antonio.cataliotti@unipa.it.

### 1. INTRODUCTION

The fast deployment of renewable generation technologies has deeply altered the structure of the electricity grid, at all voltage levels, from transmission networks to residential dwellings. In this framework, an accurate monitoring of bidirectional power flows is an essential requirement for smart grid stability [1]-[4]. Besides powers, also other quantities such as drained, injected and stored energy, current, voltage, frequency, and also power quality indexes have to be monitored. This can be obtained only by integrating modern technologies for accurate monitoring, with remote control of distributed generation (DG) and energy storage systems (ESSs), and with the support of a reliable communication infrastructure between prosumers and the Distribution System Operator (DSO). This is the well know implementation of smart grids (SGs) paradigm [5]-[6].

The capacity to establish a communication channel between the management systems of the new facilities (i.e. distributed generators and energy storage systems) and the DSO is a crucial component of this new kind of infrastructure. Several research studies on the use of different communication technologies in SGs have been presented in recent years. The authors specifically investigated the usage of power line communication (PLC) technology both on low voltage (LV) and medium voltage (MV) networks [7]-[9]. In fact, PLC is a prominent communication technology in distribution networks, because it has the key benefits of inexpensive installation cost and resilience, as it uses the power grid as the communication link. PLC is used on LV grids across the world for automatic meter reading and it has recently been proposed for other use cases such as secondary substation automation, remote control of distributed generators, and other smart grid solutions [6].

In this paper, a new architecture is proposed for smart grid deployment, which is based on the use of PLCs. The proposed architecture includes the use of two devices: a concentrator, installed in a secondary substation, and a PLC communication bridge, to be connected to the generation/storage system. Differently from previous studies of the authors, where a dedicated interface protection system (IPS) was developed according to CEI 0-21 standard [6], the communication bridge herein proposed can be connected to commercial IPS, even those already installed. Thus the proposed solution is more flexible and it could be deployed in any country, with IPS compliant to the related.

The developed new solution also embeds new features for PLC channel characterization. More in detail, signal-to-noise ratio (SNR), link quality index (LQI) and success rate are measured to obtain an efficiency estimation of PLC communication channel [10], [11]. The success rate is the ratio between the number of packets received and the number of packets sent during a communication. To maximize it, it's important to carefully choice the modulation and frequency band. In this way, the transmission parameters can be adapted to the communication channel conditions. The measurement of channel impedance is another useful factor in determining channel reliability. The impedance of an electrical network is normally determined by the network topology, connections, and types of loads connected [12]-[14]. Several literature papers report the measured impedance as a function of frequency in various power grid scenarios. In some circumstances, the channel frequency response obtained using "channel estimation" techniques is employed in real time to obtain the impedance value [15]-[17]. Measurements have also been carried out under various conditions (laboratories, urban and rural cities) [18], [19]. The experiments outcomes demonstrate that the access impedance exhibits a frequency trend that is dependent on the network topology as well as on the number and kind of connected loads. The measured impedance typically ranges from 1 to 25  $\Omega$  in metropolitan regions (made up of blocks of buildings) and from 30 to 70  $\Omega$  in rural locations. Additionally, in the latter situation, remote measurement points (i.e. far from houses) exhibit non-inductive impedance behavior. Network analyzers or measurement

devices based on data recording and processing software are used as impedance measurement techniques. One of the main disadvantages of these measurement schemes is the need for dedicated equipment and continuous knowledge of electrical networks topology. High expenses are the result of the use of specialized equipment and the difficulty of managing it. The network topology knowledge corresponds to a high quantity of data to be handled, also for the possible network reconfiguration due to connected loads changing.

In this paper, a new measurement approach is proposed, which embeds both the signal quality and the impedance measurement methods directly on the same device used for communication, i.e. the PLC modem. In this way, smart meters, which embed PLC modems, can use the same communication signal as the testing signal for channel characterization. This feature has two key benefits: 1) no dedicated measurement instrument is required, thus installation costs are reduced considerably; 2) theoretically, an impedance measurement can be made for each signal transmission. In this paper, a case study is presented based on the use of a ST8500 PLC modem. A tool has been developed to carry out a frequency characterization of the PLC signal received over the LV network. In this way, with a firmware update a smart meter can embed a channel characterization tool. Experimental laboratory tests were used to validate the measurement capabilities.

The paper is organized as follows. Section II describes the design and implementation of the new architecture and the developed devices. Section III describes the measurement methodology used for channel characterization, and especially for line impedance calculation. Section IV describes the tests for measurement instrument characterization. Finally, conclusions are drawn, and future developments are envisioned.

## 2. PROPOSED ARCHITECTURE AND DEVELOPED DEVICES

The proposed monitoring architecture for LV smart grids is shown in Fig. 1. The architecture is based on two developed devices: a concentrator, to be installed in a secondary substation, and a PLC communication bridge, to be connected to both a commercial IPS and the power converter of a generation/storage system. The bi-directional data flow for control, monitoring, and configuration signals for DGs and SSs is carried out using a hybrid PLC and Modbus-RS232 communication link. To remotely disconnect the source from the LV network, the PLC bridge can be connected to a generic interface protection system through digital pins. Moreover, it can be connected directly to an inverter of a PV source or to an Interface Electronic Device (IED). This IED is a new device which operates as a communication interface between a group of inverters of PV sources or bidirectional power converters of storage systems.

In the following, the functionalities of the two new proposed devices will be described in detail.

The concentrator has the following functions:

- Supervision of generation plants by polling inverters connected to the DGs or ESSs;
- Parsing, wrapper and router of control and management messages to and from DGs and ESSs.

The concentrator consists of two evaluation boards: the EVALKIST8500-1 and the Raspberry Pi3 that work together to develop and implement these features. The block diagram showing the connections between the two boards is shown in Fig. 2. The ST8500 PLC transceiver, which is frequently used for smart metering applications, is embedded in the evaluation board EVALKIST8500-1 [20] and it is used as link with the communication bridges connected to the related LV network. On the other hand, the concentrator can communicate with the DSO through LAN/WAN using the Ethernet interface of the Raspberry Pi3. The commands coming from the DSO are appropriately parsed and wrapped before being sent to the EVALKIST8500-1 through serial UART communication. The same steps are performed on data coming from PLC bridges of IPSs before they are delivered to the DSO. Moreover, the Raspberry Pi3, by using the same UART serial communication can act as an external host to configure the PLC communication characteristics of the EVALKIST8500-1 (i.e. modulation and frequency band). The transmission settings can then be adjusted to match the characteristics of the communication channel.

The main functions performed by the PLC bridge prototype are:

- To be able to receive distributor commands from the concentrator through the PLC link and to communicate with it to monitor, control and manage the inverters connected to DG or ESS;

- To act as communication interface with the management and control systems of DG and ESS inverters.
- To forward the remote disconnection signal sent by the DSO to a digital input of the IPS, which is able to open the contactor and disconnect the power plant from the network.

An EVALKIT8500-1 board has been used to develop and implement these features. This allows the concentrator to forward DSO commands to the IPS, DG, and ESS inverters via a PLC signal in the LV network. The DG and ESS inverters are connected via a serial connection using the Modbus/RTU protocol on RS232 to exchange data and commands. The logical level of the EVALKIT8500-1 digital output pin, which is used to transmit the remote disconnection signal to the IPS, is matched by a suitable voltage conditioning circuit. The functional diagram of the PLC bridge prototype is shown in Fig. 3.

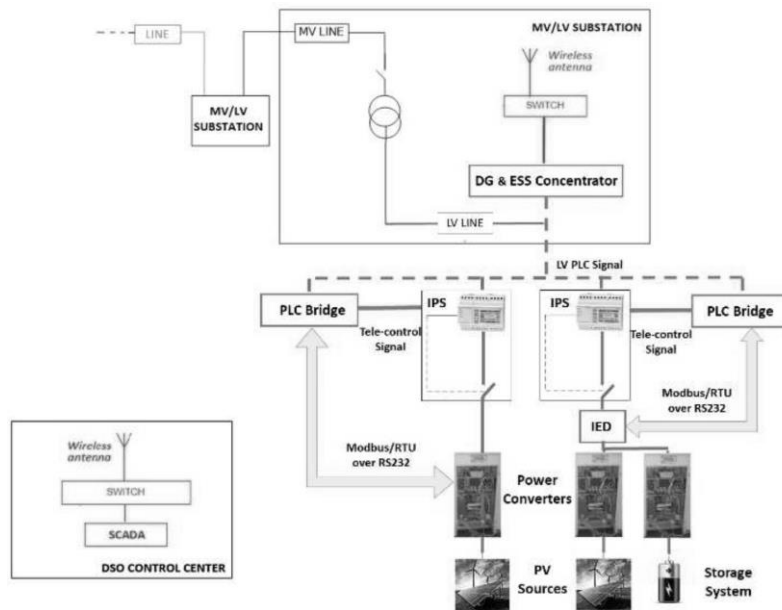


Fig. 1. Proposed PLC communication link for DG and ESS connection to LV network

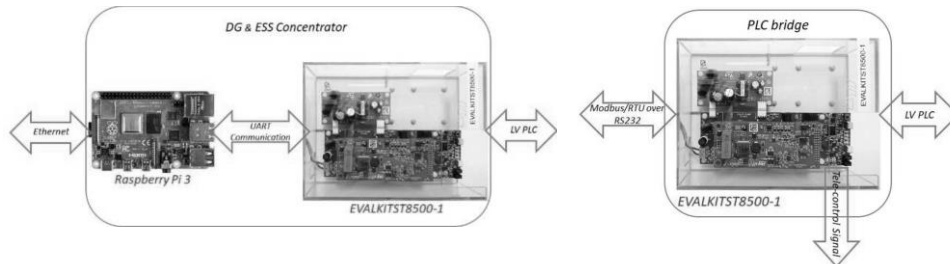


Fig. 2. Connection block diagram of DG and ESS concentrator prototype

Fig. 3. Functional diagram of PLC bridge prototype.

### 3. LINE IMPEDANCE CALCULATION

As discussed in Section II, to perform a good communication, it is important to correctly set transmission and reception parameters of the PLC transceiver. To achieve this result, it is important to measure channel characterization parameters, and in particular the line impedance. Thus in the following, a new methodology is presented for acquisition, storage, and processing of measurement data for impedance calculation in the frequency range of interest. The methodology is based on the spectrum analysis of voltage and current sampling and the calculation of network impedance at PLC

signal frequency. A novel aspect of the proposed methodology is the use of a characterization signal intrinsically present in the preamble of a PLC signal modulated with G3 protocol. A G3 PLC signal's preamble, in fact, contains all the carriers, making it possible to use it as a characterization signal. To completely understand the spectrum composition of the transmitted signal, it is helpful to refer to the standards that establish the spectral content in the various permissible frequency bands for PLC signal transmission [21] - [22].

The PLC channel has variable behavior that is strongly influenced by frequency and cable characteristics as well as the number of connected loads. In addition, it is susceptible to interference, background noise, impulse noise, and group delays of up to several hundred microseconds. OFDM modulation is specifically recommended by the standard because it's exceptionally robust in transmission in the presence of interference, noise, and frequency selective attenuation. Advanced channel coding methods are also used to guarantee coexistence with other PLC systems using the same frequency range. The band that is available for OFDM transmission is divided up into a specific number of subchannels, which are basically several independent PSK subcarriers modulated with orthogonal frequencies. The frequency-domain map of an OFDM symbol is obtained using this technique. The inverse fast Fourier transform (IFFT) is then used to transform the frequency components of the OFDM symbols so they can be represented in the time domain. In other words, the OFDM signal is generated by performing the IFFT on the complex values produced by differentially encoded phase modulation, allocated to each subcarrier. The IFFT is implemented on 256 points considering a sample frequency of 0.4 MHz for the CENELEC-A and CENELEC-B bands and 1.2 MHz for the FCC band, according to G3-PLC transceivers described in [21]. With these numbers, the subcarrier frequency spacing for the CENELEC and FCC bands, respectively, is 1.5625 kHz ( $f_s/N = 400000/256$ ) and 4.6875 kHz ( $f_s/N = 1200000/256$ ). According to [22], the IFFT is implemented on 256 points with a sample frequency of 1.2 MHz for the FCC band and 0.4 MHz for the CENELEC-A and CENELEC-B channels. With these values, the subcarrier frequency spacing is 1.5625 kHz (i.e.,  $f_s/N = 400000/256$ ) and 4.6875 kHz (i.e.,  $f_s/N = 1200000/256$ ) for CENELEC and FCC bands, respectively. According to the relative bandwidths [22], the number of usable subcarriers is 36 for the CENELEC-A band (35.9375–90.625 kHz), 16 for the CENELEC-B band (98.4375–121.875 kHz), and 72 for the FCC band (154.6875–487.5 kHz).

A typical OFDM frame on the PHY layer is made up of a preamble, a Frame Control Header (FCH), and a data section. The FCH frame contains 13 symbols, all of which perform important control functions in PHY-OFDM frame demodulation. The chosen modulation technology, such as BPSK, QPSK, 8-PSK, 16-QAM, and robust, with a coherent or differential modulation scheme, determines the payload duration in the time domain. Normally, the more robust the modulation, the longer the payload lasts in the time domain. The preamble of a generic frame, which can either contain payload data or an acknowledgment (i.e., an ACK/NACK frame without payload), is made up of eight identical SYNCP symbols, one SYNCM symbol, and half a SYNCM symbol. The difference between the SYNCM and SYNCP symbols is a shift of  $\pi$ . The whole structure of a PHY-OFDM data frame is shown in Fig. 4.

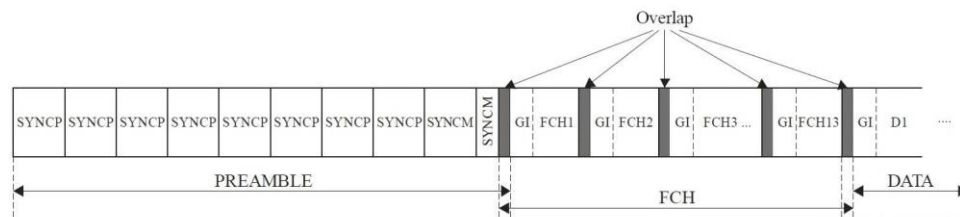


Fig. 4. PHY OFDM data frame structure.

SYNCP and SYNCM symbols are used at the start of communication to perform synchronization, channel quality assessment, and reference phase estimation. The lengths of the SYNCP and SYNCM symbols are fixed and determined by the used transmission band [21]. For transmissions in the CENELEC bands, the duration of the SYNCP/SYNCM symbol is 640  $\mu$ s, while, for transmissions in the FCC band is 213  $\mu$ s. To confirm this, Fig. 5 show the time trend of the preamble measured in the CENELEC-A band. The signal transmitted by an EVLKITST8500-1 board configured for G3-PLC

communications was the measurement's target. The signal was acquired using a Rohde & Schwarz RTO 1044 oscilloscope at a sample frequency of 200 MSa/s. Because the single SYNC/SYNCP symbol lacks any specific information, the associated OFDM signal is created by applying the IFFT to the complex-valued points that correspond to all of the subcarriers in the used transmission band. This means that the single SYNC/SYNCP symbol's spectrum content in the frequency domain is composed of several lines equal to all of the employed subcarriers. As expected, 72 subcarriers spaced at 4.6875 kHz were measured in the FCC spectrum, while 36 and 16 subcarriers spaced at 1.5625 kHz were measured in the CENELEC-A and the CENELEC-B band spectrum, respectively. The measured spectrum confirms the presence of all subcarriers and, therefore, the possibility of using this signal for channel characterization.

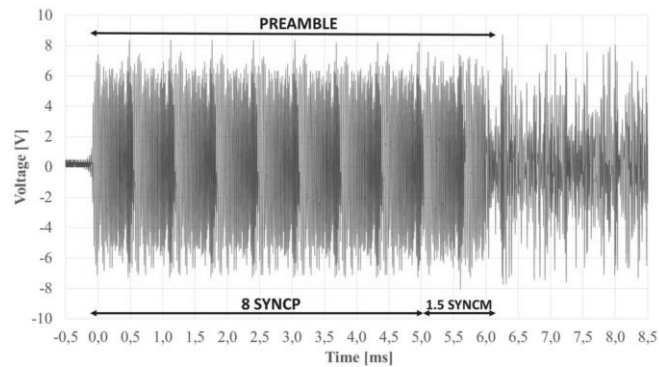


Fig. 5. OFDM preamble waveform in the CENELEC-A band.

The preliminary analysis demonstrates the properties of the OFDM signal preamble upon which the suggested impedance measurement methodology is based. In detail, the impedance value is determined by measuring voltage and current at each subcarrier. With a resolution equal to the frequency spacing between the subcarriers, the impedance frequency trend can then be determined for the entire frequency range. The impedance trend, thus, has a resolution of 1.5625 kHz for the CENELEC bands and 4.6875 kHz for the FCC band. Since the subcarriers are all contained on a single SYNC/SYNCP symbol, the observation window is equal to 640  $\mu$ s for the CENELEC band and 213  $\mu$ s for the FCC band. The higher order carrier should be considered to determine the sampling frequency. The last subcarrier is located at 90.625 kHz in the CENELEC-A band; at 121.875 kHz in the CENELEC-B band, and at 487.5 kHz in the FCC band [21]. To respect Shannon theorem, the minimum sampling frequency must be greater than 181.25, 243.75, and 975 kHz, respectively. The Complex Fast Fourier Transform (CFFT) algorithm is applied to the acquired samples to reduce the computational cost and calculation time. [23]. This algorithm can calculate the real and imaginary parts of each spectrum component. In this way, it is possible to determine the amplitude and phase of each spectral component. The FFT computation time for impedance calculation was experimentally measured as 9.4 ms, [23].

This result shows that the time variance of the impedance value can be recorded approximately in half a period of the mains voltage. The accuracy of the proposed system is lower than, for example, an ad hoc system, such as the one developed in [24], but certainly acceptable from the point of view of the hardware specifications of the low-cost commercial evaluation boards used. To implement the proposed measurement methodology, the scheme shown in [25] has been developed. It requires the usage of an EVALKITST8500-1 board for PLC signal injection, a ST NUCLEO F446RE board for impedance acquisition and calculation, and a signal conditioning board. The three boards could be combined into a single board in the future. The features and functions of the individual boards are discussed in detail below. The EVALKITST8500-1 is a modular evaluation board that consists of a motherboard and a PLC transceiver. The combined use of the two boards makes it possible to implement the line impedance calculator. This functionality has been added to the software tool developed for the EVALKITST8500-1 in [25]. More specifically, the PLC Field Analyzer tool, created in [25] for characterizing the quality of the received PLC signal, was featured under a "RX METRIC" tab in ST

Microelectronics' Smart Grid LabTool graphical user interface (GUI). To include the new capability of the line impedance calculator, the software created and used for the PLC Field Analyzer has been changed. Furthermore, the new functionality was incorporated into the same GUI under a "TX METRIC" tab. The firmware for the ST8500 has been updated to automatically configure the G3-PLC communications and to display the processed impedance values.

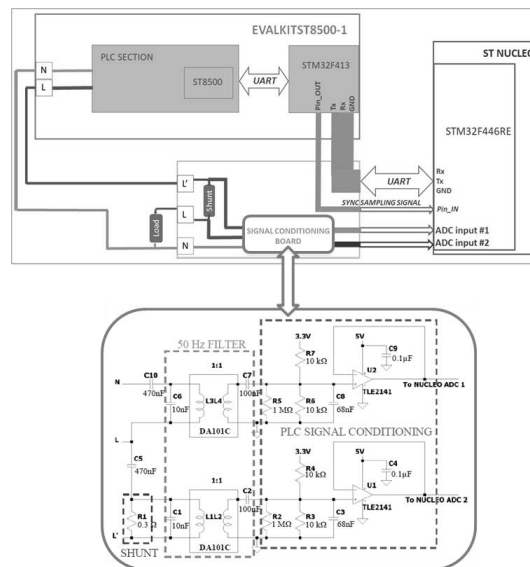


Fig. 6. Connection diagram of the boards of the line impedance calculator measurement system.

The ST-NUCLEO F446RE firmware has been developed to automatically implement the ADC configuration, run the linear CFFT algorithm and process values. The observation window was synchronized with the G3-PLC signal to sample a single SYNC symbol from the preamble using a synchronization signal provided by the EVALKITST8500-1 board. Voltage and current signals are simultaneously sampled by using two different ADCs of the STM32F446RE. More in detail, the observation window has a fixed value, equal to the single SYNC symbol duration, i.e.,  $T_w = 640 \mu\text{s}$  in the CENELEC bands, and  $T_w = 213 \mu\text{s}$  in the FCC band. The sampling frequency is determined by the last OFDM signal subcarrier. On the other hand, it should be chosen from the possible values of STM32F446RE ADCs, i.e. as a submultiple of the ADC internal clock among the selectable ones. The chosen sampling frequencies are 1.33 and 6.06 MHz for CENELEC and FCC bands, respectively. In this way, 852 samples (i.e.,  $N = T_w * f_s = 640 * 1.33$ ) are acquired for the SYNC symbol of the preamble in the CENELEC band and 1290 samples (i.e.,  $N = T_w * f_s = 213 * 6.06$ ) for the SYNC symbol in the FCC band. The digitized values transfer is performed via direct memory access (DMA) of the STM32F446RE to reduce the latency. To adapt the ADC voltage input to voltage and current signals, the signal conditioning board shown in Fig. 7 was designed and realized. It performs the following functions:

- 1) Filtering the PLC signal from the ac component at 50 Hz;
- 2) Providing a voltage signal proportional to the current signal in the whole frequency range of interest (30–500 kHz);
- 3) Adapting the signal values to the ADC input.

The different parts of the circuit are highlighted in Fig. 7 to show the correspondent functionalities. According to [26], a shunt resistor must be adjusted to a low value to reduce noise in the impedance measurement approach. On this basis, the current to voltage conversion is carried out using a  $0.3\Omega$  shunt (with a 1% accuracy) connected in series with the load.

It is possible summarize the sequence of operations carried out by the line impedance calculator as follows:

- 1) A request is sent from the “TX\_METRICS” panel of the Smart Grid LabTool (as shown in Fig. 8) to the EVALKITST8500-1, via USB, choosing one of the three transmission bands.
- 2) The EVALKITST8500-1 sends via UART a configuration message to the NUCLEO board to choose the proper sampling frequency based on the selected transmission band.
- 3) A READY status acknowledge reply is sent when the ADC configurations are complete.
- 4) The EVALKITST8500-1 starts the PLC signal transmission and sends a trigger to the ADCs in the STM32F446RE of the NUCLEO board via a digital output to start the voltage and current sampling (sync sampling signal).
- 5) When the acquisition is completed, the STM32F446RE of the NUCLEO board performs the impedance calculation by performing the spectral analysis (CFFT algorithm).
- 6) To reduce the noise, which affects voltage and current signals, the above-described PLC signal transmission–sampling–CFFT calculation sequence is performed 30 times. The mean value is then calculated for the 30 measurements performed at each carrier frequency.
- 7) The NUCLEO board transfers the impedance results to the EVALKITST8500-1 and then to the Smart Grid LabTool, which shows the results on the “TX\_METRIC” panel of Fig. 8.

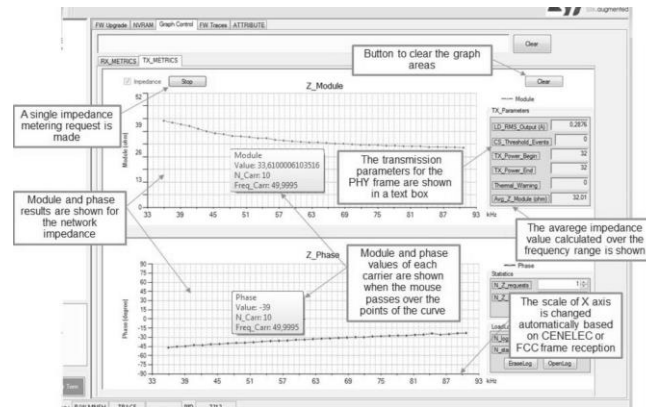


Fig. 7. Line impedance front panel on the Smart Grid LabTool.

#### 4. EXPERIMENTAL TESTS

The EVALKITST8500-1, the ST NUCLEO F446RE, and the signal conditioning circuit were used to test the line impedance calculator. The measuring system was tested by connecting loads with known values. Resistive-inductive and resistive-capacitive loads were explored in detail. The load levels were chosen to produce a typical frequency trend that might occur in a power line. The impedance values were also measured for comparison with a Keysight ENA E5080A vector network analyzer (VNA) [27]. The resolution bandwidth (RBW) of the VNA has been set to 300 Hz. Before each series of measurements, a complete one-port manual calibration was done with a Keysight 85032F calibration kit [28]. The features of the standard connectors of the calibration kit are the following: open-circuit standard with a phase uncertainty smaller than  $1.0^\circ$ ; short-circuit standard with a phase uncertainty smaller than  $1.0^\circ$ ; and match-circuit standard with a return loss higher than 48 dB. All these parameters are defined in the frequency range of 9 kHz–10 MHz. After system error correction, the accuracies of reflection measurements are 0.1 dB and  $1^\circ$  in the frequency range of the considered band. Several tests with different impedance values were carried out in all frequency ranges. As an example, Fig. 8 and Fig. 9 show the magnitude and phase results of the impedance measured with the proposed system (i.e., the line impedance calculator) in comparison with that measured by the reference instrument (the VNA). These results were obtained in a test performed in CENELEC-A band with a resistive-inductive load consisting of a  $3.3 \Omega$  resistor connected in series to a  $10 \mu\text{H}$  inductor. As it can be seen, the impedance measured by the proposed system has the same frequency trend as that measured by VNA. Mean errors of  $0.79 \Omega$  and  $2.03^\circ$  were observed over the entire frequency range in amplitude and phase measurements, respectively. These errors are compatible with the VNA accuracy specifications. Several further tests were performed both in CENELEC A, B and in FCC bands.

The results are summarized in Table I along with the different loads used in the tests. It can be seen how the measurement tool always allows to measure the impedance frequency trend with low errors, acceptable for a diagnostic tool.

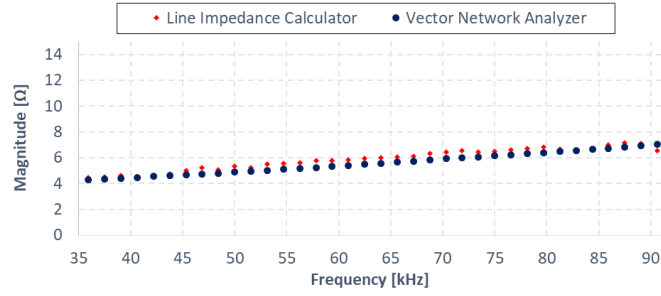


Fig. 8. Magnitude comparison between measured values by reference instrument and line impedance calculator in the case of a resistive–inductive load of  $3.3 \Omega$  and  $10 \mu\text{H}$ . Mean error =  $0.79 \Omega$ .

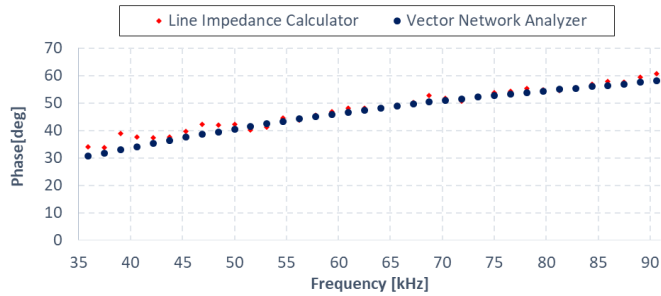


Fig. 9. Phase comparison between measured values by reference instrument and line impedance calculator in the case of a resistive–inductive load of  $3.3 \Omega$  and  $10 \mu\text{H}$ . Mean error =  $2.03^\circ$ .

Table I. Experimental Results

Frequency band	Load Impedance	Mean Errors (Magn./Phase)
CENELEC-A (35 ÷ 90 kHz)	R = $3.3 \Omega$	$0.24 \Omega$ $0.96^\circ$
	RL series R = $10 \Omega$ , L = $33 \mu\text{H}$	$0.68 \Omega$ $1.57^\circ$
	RC series R = $10 \Omega$ , C = $330 \text{ nF}$	$0.60 \Omega$ $0.37^\circ$
CENELEC-B (95 ÷ 125 kHz)	R = $10 \Omega$	$0.20 \Omega$ $1.79^\circ$
	RL series R = $24 \Omega$ , L = $100 \mu\text{H}$	$0.45 \Omega$ $1.79^\circ$
	RC series R = $24 \Omega$ , C = $15 \text{ nF}$	$1.90 \Omega$ $0.39^\circ$
FCC (150 ÷ 490 kHz)	R = $10 \Omega$	$0.16 \Omega$ $2.25^\circ$
	RL series R = $24 \Omega$ , L = $10 \mu\text{H}$	$0.99 \Omega$ $1.24^\circ$
	RC series R = $24 \Omega$ , C = $47 \text{ nF}$	$0.77 \Omega$ $1.21^\circ$

## 5. CONCLUSIONS

In this paper, new architecture and devices are proposed for the remote monitoring and control of DGs and ESSs connected to LV distribution networks. Concentrator and PLC bridge are two new sophisticated electronic devices developed to create a communication link between DSO and DGs and ESSs power converters. Moreover, new functionalities were developed to be embedded in the developed devices for PLC channel characterization. A firmware upgrade and low-cost additional hardware are used for characterization and measurement, thus avoiding the use of dedicated equipment and complex data processing software and recording hardware. In fact, a new firmware for both the received signal quality analysis (PLC Field Analyzer tool) and the power line impedance measurement was created (line impedance calculator tool). The first tool, presented in [25], allows measuring the received signal and noise levels and calculating the SNR for each carrier of the modulated signal. The second, which is described in more detail in this work, uses the same PLC signal for characterization and can determine the impedance trend of the communication channel.

The implemented measurement tools were validated through numerous experimental tests employing known values and comparing the measured values with those acquired using a reference instrument (VNA). A small difference was observed between these measurements, thus validating the measurement capability of the developed instrument. Unlike ad hoc systems, which can only take measurements on a sample basis, the proposed system, which is embedded on a single board, can perform time-varying measurements for each signal transmission. The PLC channel can be fully defined directly by the application using these two tools incorporated, for example, in a smart meter; this can considerably reduce the cost and complexity of the measurement equipment. The results obtained show that the characteristics of the diagnostic tool would be optimal for the characterization of the communication channel with connected points located at great distances, e.g., rural networks, where the value of the impedance is very high and can also have a noninductive behavior. The embedded diagnostic tool could be also used to locate possible frequency bands with a higher level of attenuation or noise and to choose the proper frequency bands for optimal transmission. The described procedures can be executed as a diagnostic tool for an operator who wants to investigate the network behavior via the Smart Grid LabTool.

However, in future work, these procedures could be performed also automatically at each signal transmission; the obtained impedance values could be then stored for post diagnosis, or they can be used to periodically adapt the transmission frequencies to the channel behavior.

## 6. ACKNOWLEDGEMENT

The research received the financial support of the European Union in the following grants: Program IEV CT Italie Tunisie 2014-2020, Project n. IS\_2.1\_131, Project acronym: SInERT, CUP: B74I19001040006 and B74I18014130002, Project title: "Solution innovantes pour l'intégration des énergies renouvelables sur le réseau électrique tunisien". The paper content is solely responsibility of the authors and it does not necessarily reflect the point of view of the European Union.

The authors wish to thank engineers of STMicroelectronics laboratory of Rennes, France, for their scientific support.

## RIFERIMENTI BIBLIOGRAFICI

- [1] F. Bonavolontà, L. P. Di Noia, D. Lauria, A. Liccardo, and S. Tessitore, "An Optimized HT-Based Method for the Analysis of Inter-Area Oscillations on Electrical Systems," *Energies*, vol. 12, no. 15, p. 2935, Jul. 2019.
- [2] A. Maalej and C. Rebai, "Sensor Data Augmentation Strategy for Load Forecasting in Smart Grid Context," *2021 18th International Multi-Conference on Systems, Signals & Devices (SSD)*, 2021, pp. 979-983.
- [3] G. D'Avanzo, A. Delle Femine, D. Gallo, C. Landi, M. Luiso, "Impact of inductive current transformers on synchrophasor measurement in presence of modulations", *Measurement*, Volume 155, 2020.
- [4] G. Crotti, D. Giordano, G. D'Avanzo, P.S. Letizia, M. Luiso, "A New Industry-Oriented Technique for the Wideband Characterization of Voltage Transformers", *Measurement*, Volume 182, 2021.
- [5] A. Rosato, M. Panella, R. Araneo and A. Andreotti, "A Neural Network Based Prediction System of Distributed Generation for the Management of Microgrids," in *IEEE Transactions on Industry Applications*, vol. 55, no. 6, pp. 7092-7102, Nov.-Dec. 2019.

- [6] A. Cataliotti, V. Cosentino, D. Di Cara, S. Guaiana, N. Panzavecchia, G. Tine, "A New Solution for Low-Voltage Distributed Generation Interface Protection System," *IEEE Transactions on Instrumentation and Measurement*, vol. 64, no. 8, pp. 2086-2095, Aug. 2015.
- [7] G. Artale, A. Cataliotti, V. Cosentino, D. Di Cara, R. Fiorelli, S. Guaiana, N. Panzavecchia, G. Tinè, "A new low cost power line communication solution for smart grid monitoring and management", *IEEE Instrum. & Meas. Magazine*, vol. 21, no. 2, pp. 29-33, April 2018.
- [8] G. Artale, A. Cataliotti, V. Cosentino, D. Di Cara, R. Fiorelli, S. Guaiana, G. Tinè, "A New Low Cost Coupling System for Power Line Communication on Medium Voltage Smart grids," *IEEE Trans. on Smart Grid*, vol. 9, no. 4, pp. 3321-3329, July 2018
- [9] G. Artale, A. Cataliotti, V. Cosentino, D. Di Cara, R. Fiorelli, S. Guaiana, N. Panzavecchia, G. Tinè, "A New PLC-based Smart Metering Architecture for Medium/Low Voltage Grids: Feasibility and Experimental Characterization" *Measurement* 129 (2018) 479–488.
- [10] G. Chu, J. Li, and W. Liu, "Narrow band power line channel characteristics for low voltage access network in China," in *Proc. IEEE 17th Int. Symp. Power Line Commun. Appl.*, Mar. 2013, pp. 297–302.
- [11] C. M. De Dominicis, A. Flammini, S. Rinaldi, M. Rizzi, and A. Vezzoli, "Characterization of multi-standard power line communication on lowvoltage grid," in *Proc. IEEE Int. Instrum. Meas. Technol. Conf. (I2MTC)*, May 2013, pp. 31–36.
- [12] F. Passerini and A. M. Tonello, "Smart grid monitoring using power line modems: Anomaly detection and localization," *IEEE Trans. Smart Grid*, vol. 10, no. 6, pp. 6178–6186, Nov. 2019.
- [13] F. Passerini and A. M. Tonello, "Power line fault detection and localization using high frequency impedance measurement," in *Proc. IEEE Int. Symp. Power Line Commun. Appl. (ISPLC)*, 2017, pp. 1–5.
- [14] Y. Huo, G. Prasad, L. Atanackovic, L. Lampe, and V. C. M. Leung, "Grid surveillance and diagnostics using power line communications," in *Proc. IEEE Int. Symp. Power Line Commun. Appl. (ISPLC)*, Apr. 2018, pp. 1–6.
- [15] D. Liang, S. Ge, H. Guo, Y. Wang, Z. Liang, and C. Chen, "Monitoring power line faults using impedance estimation algorithms in power line communication equipment," in *Proc. 10th Int. Conf. Power Energy Syst. (ICPES)*, Dec. 2020, pp. 404–408.
- [16] D. Liang, H. Guo, and T. Zheng, "Real-time impedance estimation for power line communication," *IEEE Access*, vol. 7, pp. 88107–88115, 2019.
- [17] D. Liang, H. Guo, and T. Zheng, "Impedance tracking and estimation using power line communications," in *Proc. IEEE Int. Symp. Power Line Commun. Appl. (ISPLC)*, Apr. 2019, pp. 1–6.
- [18] L. Capponi, I. Fernandez, D. Roggo, A. Arrinda, I. Angulo, and D. De La Vega, "Comparison of measurement methods of grid impedance for narrow band-PLC up to 500 kHz," in *Proc. IEEE 9th Int. Workshop Appl. Meas. Power Syst. (AMPS)*, Sep. 2018, pp. 1–6.
- [19] I. Fernández, A. Arrinda, I. Angulo, D. D. L. Vega, N. Uribe-Pérez, and A. Llano, "Field trials for the empirical characterization of the low voltage grid access impedance from 35 kHz to 500 kHz," *IEEE Access*, vol. 7, pp. 85786–85795, 2019.
- [20] G. Artale *et al.*, "Implementation of a PLC Field Analyzer on a G3 Modem Platform", IEEE International Instrumentation & Measurement Technology Conference, Virtual Conference, May 17-20, 2021.
- [21] *Narrowband Orthogonal Frequency Division Multiplexing Power Line Communication Transceivers–Power Spectral Density Specification*, Recommendation, document ITU-T G 9901.
- [22] *Narrowband Orthogonal Frequency Division Multiplexing Power Line Communication Transceivers for G3-PLC Networks*, Recommendation, document ITU-T G 9903, Aug. 2017.
- [23] G. Artale *et al.*, "PQ and harmonic assessment issues on low-cost smart metering platforms: A case study," *Sensors*, vol. 20, no. 21, p. 6361, Nov. 2020.
- [24] C. Nieb, J.-P. Kitzig, and G. Bumiller, "Measurement system for time variable subcycle impedance on power lines," in *Proc. IEEE Int. Instrum. Meas. Technol. Conf. (I2MTC)*, May 2021, pp. 1–6.
- [25] G. Artale *et al.*, "Implementation of a PLC field analyzer on a G3 modem platform," in *Proc. IEEE Int. Instrum. Meas. Technol. Conf. (I2MTC)*, May 2021, pp. 1–3.
- [26] F. Passerini and A. M. Tonello, "Analysis of high-frequency impedance measurement techniques for power line network sensing," *IEEE Sensors J.*, vol. 17, no. 23, pp. 7630–7640, Dec. 2017.
- [27] *E5080A ENA Vector Network Analyzer, Data Sheet 5992-0291EN*, Keysight Technologies, Santa Rosa, CA, USA. Accessed: Jun. 26, 2020. [Online]. Available: <https://www.keysight.com/it/en/assets/7018-04644/data-sheets/5992-0291.pdf>
- [28] *Keysight 85032F Type-N 50 Calibration Kit, User's and Service Guide*, Keysight Technologies, Santa Rosa, CA, USA. Accessed: Feb. 3, 2022. [Online]. Available: <https://www.keysight.com/it/en/assets/9018-01295/user-manuals/9018-01295.pdf>